# Shear-Induced Phase Separation in Aqueous Polymer Solutions: Temperature-Sensitive Microgels and Linear Polymer Chains

**Markus Stieger and Walter Richtering***

*Institute of Physical Chemistry, Christian-Albrechts-University of Kiel, Olshausenstr. 40, D-24098 Kiel, Germany*

*Received June 10, 2003; Revised Manuscript Received September 11, 2003*

ABSTRACT: The influence of shear flow on the phase separation of aqueous poly(*N*-isopropylacrylamide) (PNiPAM) microgel suspensions was investigated by means of rheo-turbidity and rheo-small angle neutron scattering (rheo-SANS) and compared to the behavior of linear PNiPAM macromolecules. The rheological behavior of concentrated microgel suspensions depends strongly on temperature, but flow and viscoelastic properties of concentrated solutions of the linear polymer are not significantly affected by temperature changes. Shear-induced phase separation was observed for both polymer architectures, although the viscoelastic properties of the two systems have different structural origins. Shear-induced demixing was found with a microgel with a cross-linking density of 1.5 mol % only at high concentrations when the sample behaved as a viscoelastic solid near the equilibrium demixing temperature. No influence of shear flow on the miscibility gap was observed for a PNiPAM microgel with a higher cross-linking density (5.5 mol %). This indicates that a coupling of shear stress with the concentration fluctuations leading to solvent squeezing is only possible when the particles are densely packed and sufficiently soft.

## 1. Introduction

A characteristic feature of many aqueous polymer solutions is that phase separation can occur upon heating. The temperature minimum of the miscibility gap is known as the lower critical solution temperature (LCST). Polymer solutions in organic solvents usually display an upper critical solution temperature (UCST) and demix upon cooling. Prominent examples for water-soluble polymers displaying a LCST are poly(*N*-isopropylacrylamide) (PNiPAM),[1] methylhydroxypropylcellulose (MHPC),[2] and poly(vinylcaprolactam) (PVCa).[3]

Temperature-sensitive PNiPAM polymers gained great interest due to their potential use in many technological applications, including drug delivery systems and biotechnology.[1,4,6] PNiPAM is known to undergo a temperature-induced phase transition in water at the LCST of 31−34 °C. The solvent quality changes from good to poor when the temperature is increased, eventually leading to phase separation. The phase transition was studied in great detail for polymers with different molecular architectures, including solutions of linear chain PNiPAM, chemically cross-linked microgels, and macroscopic gels.[1,5,6] For single linear PNiPAM, the flexible polymer chain contracts with increasing temperature, and a coil-to-globule transition is observed. Cross-linked microgels and macrogels exhibit a volume phase transition from a highly swollen to a collapsed state at elevated temperatures. It has been shown that the volume phase transition can be induced by temperature, pressure, and solvent composition. The transition temperature can be altered by addition of salt[7] or surfactants,[8] by variations in the solvent quality,[9] or by copolymerization with charged monomers.[10]

It is well-known that shear flow can influence the phase separation of polymer solutions.[11] There are several reports on the behavior of poly(styrene) (PS) dissolved in dioctylphthalate (DOP) using different techniques to probe the demixing process including turbidity, dichroism, small-angle light scattering (SALS), and small-angle neutron scattering (SANS). Recent papers by Hashimoto and Boué et al. provide a thorough review of this system.[12−14] Often a so-called butterfly pattern in SALS and SANS is observed under shear flow, indicating shear-induced concentration fluctuations. The butterfly pattern is usually observed with semidilute solutions above the overlap concentration, indicating that entanglements are necessary for the enhancement of concentration fluctuations along the flow direction. Butterfly scattering patterns have also been observed with polymer networks and some colloidal systems.[15−19] It has been pointed out that viscoelastic properties, the first normal stress difference in particular, play an important role for the coupling between density fluctuations and shear stress.[20] The presence of an entanglement network appears to be unnecessary for the shear-induced fluctuations, since experiments in dilute polymer solutions reveal that shear-induced aggregation can occur.[21]

Much less is known about aqueous solutions where phase separation occurs upon heating. Recently, Wolf and co-workers investigated aqueous solutions of hydrophobically modified ethylhydroxyethylcellulose, which also show LCST behavior.[22] Turbidity measurements revealed a strong influence of shear flow on the phase separation. With increasing shear rate the cloud temperature was shifted to higher values. It was concluded that the shear-induced mixing is due to a destruction of intersegmental clusters, which are formed via the hydrophobic side chains. MHPC solutions demonstrate a very complex behavior, revealing shear induced mixing at low concentrations but demixing at higher concentrations.[23] Badiger et al.[24] observed shear-induced demixing in aqueous solutions of high molecular weight PNiPAM solutions. Compared to the quiescent state, the linear chain polymer solutions entered the two-phase region at lower temperatures when shear flow was applied. The authors attribute the shift of the cloud

* To whom correspondence should be sent: e-mail richtering@rwth-aachen.de.

10.1021/ma034788s CCC: $25.00 
Published on Web 10/22/2003

point temperature to the destruction of intersegmental clusters formed in the stagnant state. A stress overshoot is observed for concentrated solutions before the onset of steady shear flow, indicating the existence of clusters.

Most investigations employed solutions of linear chain macromolecules above the overlap concentration. Thus, the microstructure is characterized as a highly entangled polymer solution. Shear-induced phase separation can be interpreted in different ways. Wolf suggested a general thermodynamic approach.[25] In addition to the usual Flory−Huggins−Gibbs energy of polymer solutions, a second term is introduced, the stored elastic energy. In the case of dilute polymer solutions the stored elasticity accounts for coil stretching. Other approaches describe the dynamic coupling between concentration fluctuations and stress.[26−28] Semidilute polymer solutions can be characterized by a typical correlation length and longest relaxation time of the entangled chains. In the strong shear regime of high shear rates, the stress can be released by squeezing solvent from the more entangled regions, thus enhancing concentration fluctuations. In colloidal systems shear flow can also lead to aggregation, flocculation, and different structures; for example, the formation of large-scale bundle ordering has been observed.[29]

The microstructures of colloidal and polymer solutions are very different. Thus, different properties near the miscibility gap can be anticipated. However, very little is known about the influence of the macromolecular architecture on the phase separation behavior under shear. In the present study we investigated the flow behavior and the viscoelastic properties of linear chain PNiPAM solutions as well as of concentrated PNiPAM microgel suspensions for various temperatures. The influence of shear flow on the phase separation was studied for both polymer architectures. Phase separation was monitored by rheo-turbidity measurements. Cloud point temperature curves will be presented for both polymer architectures at rest and under sheared conditions. Small-angle neutron scattering experiments under shear (rheo-SANS) were performed in order to determine the flow-induced structures. Preliminary results of the rheo-SANS investigations are included in this contribution.

## 2. Experimental Part

**2.1. Synthesis.** The preparation of the linear chain PNiPAM is based on the procedure described by Meewes et al.[30,31] The monomer *N*-isopropylacrylamide NiPAM (204.0 g, Aldrich) was purified by recrystallization from a 50 wt % benzene−hexane solution (324.0 g). An aqueous solution of hydrogen peroxide $H_2O_2$ (30 wt %, Merck), argon (99.998%), and pure methanol were used as received. NiPAM (100.0 g) was dissolved in 2000 mL of pure water at 25 °C. The polymerization vessel was evacuated and filled with argon. The $H_2O_2$ (1 mL) was added, and the reaction mixture was degassed again. The polymerization was started by opening the shutter of the UV lamp (Osram mercury vapor lamp Hg-10) and stopped after 35 min by closing the shutter and aerating the solution. The reaction mixture was poured into cold methanol and was heated slowly to room temperature. A fine precipitate of PNiPAM was decanted. For further purification, the polymer was dissolved in methanol and cold water was added. The precipitate was decanted, and another purification cycle was performed. Finally, the polymer was dissolved in water and isolated by freeze-drying.

The PNiPAM microgel particles were prepared as described previously,[32] but different quantities of the reagents were employed in order to obtain particles with larger radii (NiPAM, 23.19 g; *N*,*N*′-methylenbis(acrylamide), 0.48 g; sodium dodecyl sulfate, 0.014 g; potassium peroxodisulfate, 0.96 g). For purification the dispersion was filtered followed by extensive dialysis against pure water for 20 days.

**Table 1. Radius of Gyration $R_g$, Second Virial Coefficient $A_2$, and Overlap Concentration $c^*$ for Solutions of Linear Chain PNiPAM at Different Temperatures Determined by SLS**

| $T$/°C | $R_g$/nm | $A_2$/mol × cm$^3$/g$^2$ | $c^*$/wt % |
|---|---|---|---|
| 22.2 | 115 ± 3 | $1.4 \times 10^{-4} \pm 8 \times 10^{-6}$ | 0.1 |
| 25.8 | 114 ± 1 | $1.2 \times 10^{-4} \pm 3 \times 10^{-6}$ | 0.1 |
| 30.3 | 97 ± 2 | $5.0 \times 10^{-5} \pm 4 \times 10^{-6}$ | 0.1 |
| 33.7 | 89 ± 2 | $1.8 \times 10^{-5} \pm 4 \times 10^{-6}$ | 0.2 |
| 35.8 | 78 ± 2 | $-9.3 \times 10^{-7} \pm 2 \times 10^{-8}$ | 0.3 |
| 36.5 | 65 ± 3 | $-1.0 \times 10^{-6} \pm 2 \times 10^{-8}$ | 0.6 |

**2.2. Experimental Details.** Static light scattering experiments (SLS) were performed using a computer-controlled modified FICA goniometer with a helium−neon ion laser at a wavelength of $\lambda_0 = 632.8$ nm. The polymer solutions were filtered (MembraPure, pore size 0.2 $\mu$m) and diluted, resulting in concentrations ranging from 0.05 to 0.5 mg/mL. The intensity of the scattered light was monitored from 30° to 145° in steps of 5°. For the refractive index increment at 25 °C $dn/dc = 0.162$ mL/g was used at $\lambda_0 = 632.8$ nm.[33]

The rheological experiments were performed with a Bohlin CS-10 rheometer using a cone and plate shear geometry (1°/40 mm) made of aluminum.

For the rheo-optical experiments a modified Bohlin CVO-120-HR rheometer was used with a cone and plane shear geometry (1°/40 mm) made of quartz glass. The light of a HeNe laser ($\lambda = 632.8$ nm) passes through the sample along the velocity gradient direction, and the transmitted intensity is measured by a photodiode. The signal of the photodiode is amplified and recorded by a computer. The temperature and shear rate dependent transmitted intensity, $I_t$, was normalized by the intensity at low temperatures, $I_0$, when the sample was in the stable one-phase region. The turbidity $\alpha$ was obtained from the ratio of the normalized intensities and the sample thickness $L = 0.3$ mm as $\alpha = (-1/L) \ln(I_t/I_0)$. A detailed description of the apparatus is provided in the literature.[34]

Small-angle neutron scattering experiments under shear were performed at the instrument D11 of the Institute Laue-Langevin (ILL) in Grenoble, France. The neutron wavelength was $\lambda = 12$ Å with a spread of $\Delta\lambda/\lambda = 9\%$. The data were corrected for background and empty cell scattering, and the incoherent scattering of $H_2O$ was used for absolute calibration. A Bohlin CVO-120-HR rheometer was adjusted to the D11 beamline. Measurements were performed using a Searle shear cell consisting of quartz cylinders with a gap of 1 mm. The scattering experiments were performed in the radial position, yielding information in the plane formed by flow and vorticity direction.

## 3. Results and Discussion

**3.1. Static Light Scattering of the Linear Chain PNiPAM and the PNiPAM Microgel.** The coil-to-globule transition of very dilute solutions of linear chain PNiPAM in water has been studied intensely.[35,36] To determine molecular weight $M_w$, radius of gyration $R_g = \langle s^2 \rangle_z^{0.5}$, and second virial coefficient $A_2$, static light scattering experiments in dilute solution were performed with the linear chain PNiPAM. From the extrapolation of $Kc/R(q)$ to zero angle and zero concentration in the Zimm plots $R_g$ and $A_2$ were determined. The weight-average molar mass $M_w = 3.9 \times 10^6$ g/mol was obtained, and the overlap concentration $c^*$ given by $c^* = 3M_w/4\pi R_g^3 N_L$ was calculated. The temperature dependence of $A_2$, $R_g$, and $c^*$ is summarized in Table 1.

$A_2$ and $R_g$ remain nearly unchanged in the temperature range between 22 and 26 °C. At temperatures above 26 °C, $A_2$ and $R_g$ decrease with increasing

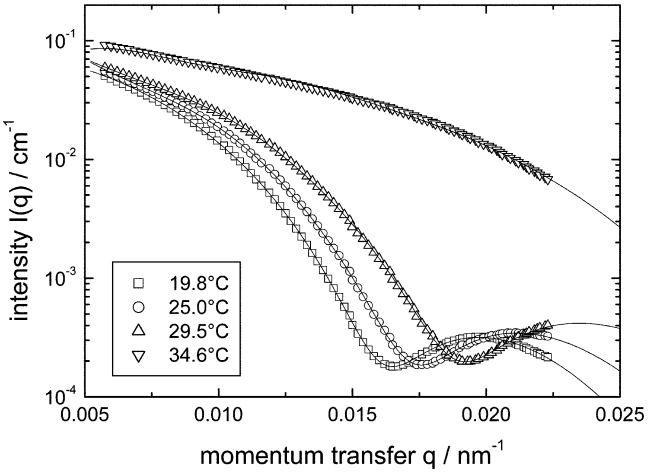


**Figure 1.** Static light scattering intensity from the PNiPAM microgel at a concentration of 0.126 g/L in $D_2O$ at different temperatures. The lines represent fits with a form factor model (see text).

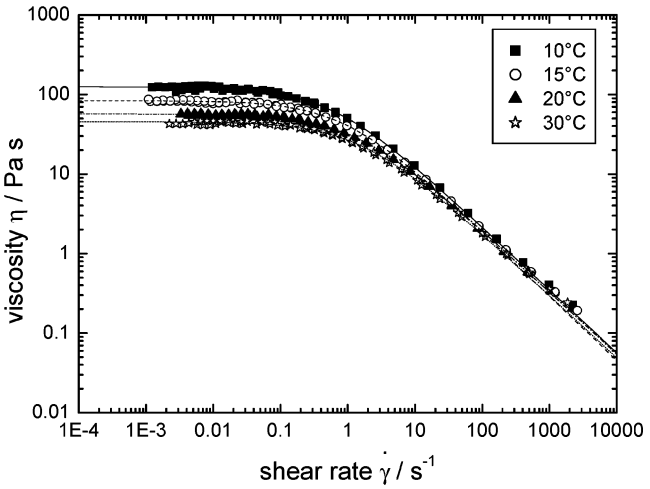


**Figure 2.** Viscosity as a function of shear rate for different temperatures for the linear chain PNiPAM in $D_2O$ at a concentration of 4.7 wt %. The lines represent fits according to the equation given by Cross.[41]

temperature due to the changes in solvent quality from good to poor. At temperatures above the $\theta$-temperature negative values for the second virial coefficient are found, and the radius of gyration declined dramatically. The overlap concentration $c^*$ increases slightly with increasing temperature.

Figure 1 shows the static light scattering intensity obtained from very dilute suspensions of the PNiPAM microgel (0.0126 wt %) at four temperatures. A shift of the form factor minima to higher $q$ values and the decrease of the initial slope of the scattering profiles in the low-$q$ regime confirm the apparent shrinkage of the particles with rising temperature. From SLS experiments the particle radius and the size distribution can be obtained by fitting the intensity profile with a model expression of the form factor. For a homogeneous sphere with a box-shaped radial scattering length density distribution, the form factor did not describe the experimental data at temperatures below the LCST.[37] Obviously, the polymer network of the cross-linked microgel particles exhibits inhomogeneous segment density in the highly swollen state which have to be included in the model expression. The form factor of a sphere with a scattering length distribution that gradually decreases at the sphere interface following a half-Gaussian distribution[38] fitted the experimental data very well for all temperatures. In this manner, particle radii of $R$(19.8 °C) = 355 nm, $R$(25.0 °C) = 325 nm, $R$(29.5 °C) = 279 nm, and $R$(34.6 °C) = 155 nm as well as a relative particle size polydispersity of 9% at 25 °C were found.

**3.2. Rheology of Concentrated Solutions of Linear Chain PNiPAM.** Unless otherwise stated, all rheological investigations were carried out using heavy water ($D_2O$) as a solvent for the linear polymer and the microgels to facilitate comparison to SANS. Preliminary results of SANS experiments on the influence of shear on the miscibility gap will be presented in this article. A detailed analysis of the rheo-SANS investigations will be discussed later. According to Shirota et al.,[39] the phase transition temperature increases by 1 K when $D_2O$ is used instead of $H_2O$.

Figure 2 displays flow curves representative of concentrated solutions (4.7 wt %) of the linear PNiPAM polymer in $D_2O$. The flow curves are characterized by a clear zero shear plateau $\eta_0$ at low shear rates and strong shear thinning at higher shear rates. However, there is only a small influence of temperature on the viscosity. Changing the temperature from 10 to 30 °C gives rise to a decrease of $\eta_0$ by a factor of 2.7 from $\eta_0 = 124$ Pa s to $\eta_0 = 46$ Pa s. In the shear thinning regime no influence of the temperature on the viscosity can be detected. The high molar mass macromolecules form a highly entangled polymer solution at concentrations well above the overlap concentration. Such solutions are not very sensitive to changes in the size of the individual macromolecules, as long as the concentration stays well above the overlap concentration. The viscoelastic properties do not reveal a pronounced temperature dependence either. The steady-state viscosity $\eta$ and the dynamic complex viscosity $\eta^*$ as a function of shear rate $\dot{\gamma}$ and angular frequency $\omega$, respectively, coincide on a single curve for all temperatures, revealing that the Cox−Merz rule[40] applies. These results indicate that the rheological behavior is determined by the mechanical interactions of the entangled network. Apparently, the influence of specific physical or chemical interactions is negligible.

The experimental flow curves were fitted using an expression given by Cross[41]

$$\frac{\eta}{\eta_0} = \frac{1}{1 + (\tau\dot{\gamma})^n} \tag{1}$$

which is known to provide a good description of the viscosity of concentrated polymer solutions. Zero shear viscosity $\eta_0$, relaxation time $\tau$, and power law exponent $n$ were obtained for various concentrations and temperatures. For the 4.7 wt % microgel suspension shown in Figure 2, a power law exponent $n = 0.78$ was obtained for all temperatures. The concentration and temperature dependence of $\eta_0$ is given in Figure 3. The course of the viscosity as a function of concentration is similar for all temperatures. At low concentrations the viscosity increases slightly with increasing concentration. At concentrations above the overlap concentration $c^*$ a strong dependence of $\eta_0$ on $c$ is observed.

At concentrations well above $c^*$, a power law behavior of $\eta_0 \propto c^q$ is observed. That corresponds to a scaling behavior of the specific viscosity $\eta_{spec} \propto (c[\eta])^q$ for large values of $c[\eta]$ with the intrinsic viscosity $[\eta] \approx 1/c^*$.

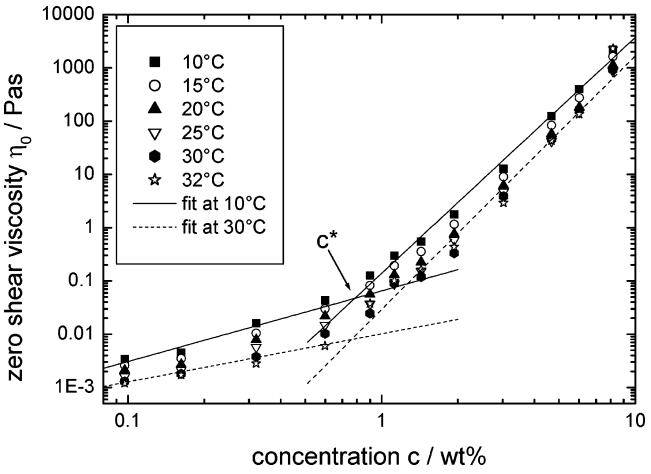


**Figure 3.** Zero shear viscosity as a function of concentration for different temperatures for the linear chain PNiPAM in $D_2O$. The lines represent power law fits to the 10 and 30 °C data at low (0.1−0.6 wt %) and at high concentrations (0.9−8.2 wt %), respectively.

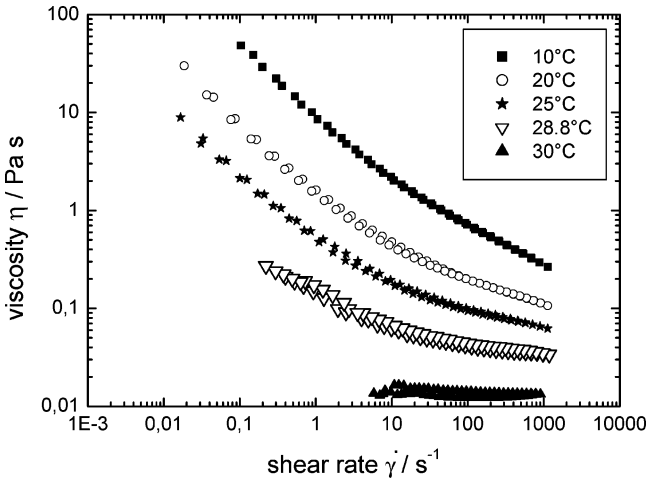


**Figure 4.** Viscosity as a function of shear rate for different temperatures for the PNiPAM microgel in $D_2O$ at a concentration of 5.1 wt %.

Since $[\eta]$ is related to the molecular weight by the Mark−Houwink−Sakurada equation $[\eta] = K_v M^{\alpha}$, a power law behavior of $\eta_{spec} \propto c^q M^{q\alpha}$ is obtained. For high molecular weight polymer melts an exponent of $q\alpha = 3.4$ is expected. For undisturbed polymer coils in polymer melts, $\alpha = 0.5$ is found. Therefore, $\eta_{spec}$ of concentrated polymer $\theta$-solutions at high $c[\eta]$ values reveal a $c^{6.8}$ dependence. Nondraining polymer coils in a good solvent with $\alpha = 0.764$ exhibit an increase to $\eta_{spec} \propto c^{4.45}$. These scaling concepts should hold for all polymers regardless of their chemical composition.[42] For the temperature-sensitive linear chain PNiPAM we observed an increase of $q$ with increasing temperature. At low temperatures (10 °C) a value of $q = 4.5$ indicates good solvent conditions that become worse at elevated temperatures. At 20 °C the exponent $q = 4.7$ and at 30 °C $q = 5.3$ were obtained. At higher temperatures (32 °C) the exponent $q = 5.6$ is still below $q = 6.8$ for $\theta$-polymer solutions, since the temperature is still below the $\theta$-temperature. The temperature dependence of the power law exponents of concentrated polymer solutions agrees well with the decrease of the second virial coefficient $A_2$ with heating we observed in dilute solution by SLS.

A power law behavior of the relaxation times $\tau$ obtained from the Cross fits with concentration is observed for all temperatures ($\tau \propto c^n$). At high concentrations $\tau$ is nearly temperature-independent since the relaxation process of the polymer chain is determined by the relaxation of the entangled network. In contrast, $\tau$ is temperature dependent at lower concentrations, and a decrease of $\tau$ is observed with increasing temperature. The temperature-dependent size of the polymer coil influences the relaxation behavior more strongly when the network is not highly entangled. The power law exponents $n$ increase with rising temperature, indicating a slight decrease in entanglements. At low temperatures (10 °C) we observed a slope of $n = 3.1$; at 20 °C $n = 3.3$ and at 32 °C $n = 3.9$ were obtained.

**3.3. Rheology of the PNiPAM Microgel.** Flow curves representative of concentrated PNIPAM microgel suspensions (5.1 wt %) are displayed in Figure 4. Shear thinning is observed, and the microgel sample reveals a strong influence of temperature on the flow behavior. The viscosity decreases by 2−3 orders of magnitude when the temperature is raised from 10 to 30 °C. This behavior is caused by the strong dependence of the size of the microgel particles on temperature. It has been shown before that the effective volume fraction of the microgel particles decreases with temperature, and a master curve of the zero shear viscosity is obtained when the effective volume fraction is used as concentration parameter.[32] For the microgel investigated in this study a sufficient number of zero shear viscosities required to obtain a master curve could not be experimentally observed since the radius of the microgel employed in these studies is large. The dimensionless Peclet number

$$P_e \equiv \dot{\gamma} t_D = \dot{\gamma} \frac{6\pi\eta_s a^3}{k_B T} \qquad (2)$$

relates the shear rate $\dot{\gamma}$ with the time $t_D$ for a particle to diffuse a distance equal to its radius $a$ in a solvent of viscosity $\eta_s$. A plateau in $\eta_0$ can only be observed when the applied shear rate does not disturb the equilibrium distribution of interparticle spacings. For the large particles the low shear rate limit of $P_e < 1$ was out of the experimentally accessible range.

The different temperature sensitivity of concentrated microgel suspensions as compared to that of linear polymer solutions is due to the different microstructure. An entangled network is present in the former whereas a close-packed structure of spheres is formed in the later. This gives rise to a strong temperature sensitivity of the flow and the viscoelastic behavior of the microgel suspensions whereas solutions of the linear chain PNiPAM exhibit no significant temperature dependence of the rheological behavior.

**3.4. Shear-Induced Demixing.** A convenient technique to study phase separation of polymer solutions is to measure the optical transmission. Usually the solution is sheared at a constant shear rate, and the transmitted light intensity is determined as the temperature is increased. In our experiments a heating rate of 0.1 K/min was used. The turbidity obtained from two microgel suspensions at concentrations of 8.0 and 10.0 wt % at varied shear rates is shown in Figure 5.

Both samples became turbid with increasing temperature; however, a shear-induced shift of the curve was only observed in the concentrated sample. The shift of

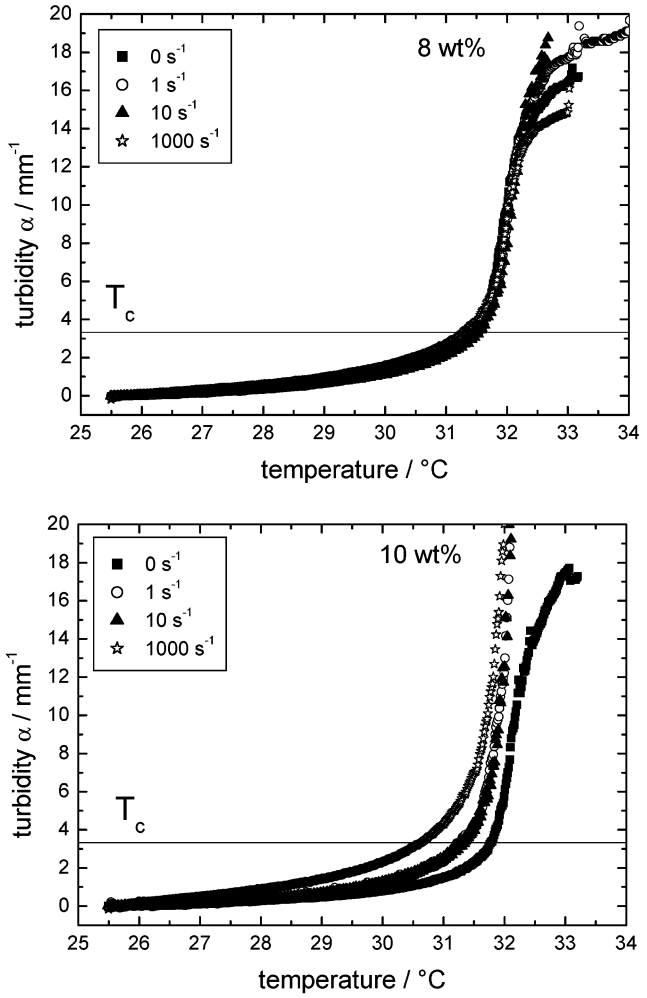


**Figure 5.** Turbidity as a function of temperature for a 8.0 wt % (top) and a 10.0 wt % (bottom) PNiPAM microgel suspension. An influence of shear flow on $T_c$ is only observed for the 10.0 wt % microgel.

the turbidity curve to lower temperatures at a higher shear rate demonstrates that shear flow caused phase separation at lower temperature relative to the quiescent state. The turbidity curves can be characterized by the cloud point temperature $T_c$. In this study we defined $T_c$ as the temperature corresponding to a developing turbidity of $\alpha = 3.33$ mm$^{-1}$, or a transmission of $I_t/I_0 = 1/e = 0.368$, as indicated in the figures.

The behavior of a solution of the linear PNiPAM at a concentration of 4.0 wt % is shown in Figure 6. Again, shear-induced phase separation is observed. The shear-induced shift of the turbidity curve is more pronounced than in the microgel samples.

In addition, isothermal rheo-optical experiments were performed with the linear chain polymer (4.7 wt %) at temperatures approximately 1 K below $T_c$ in the quiescent state (32.7 °C). The sample was presheared at $\dot{\gamma} = 5$ s$^{-1}$ for 10 min. Then a shear rate of $\dot{\gamma} = 1000$ s$^{-1}$ was applied for 2 min. A strong turbidity developed immediately after the high shear rate was applied, indicating shear-induced demixing. After reduction of the shear rate to $\dot{\gamma} = 5$ s$^{-1}$ the sample became transparent immediately, indicating that the shear-induced phase transition is reversible. Isothermal experiments were performed with the microgel (10.0 wt %) as well, and similar results were obtained. These experiments revealed again that the shear flow induces a phase

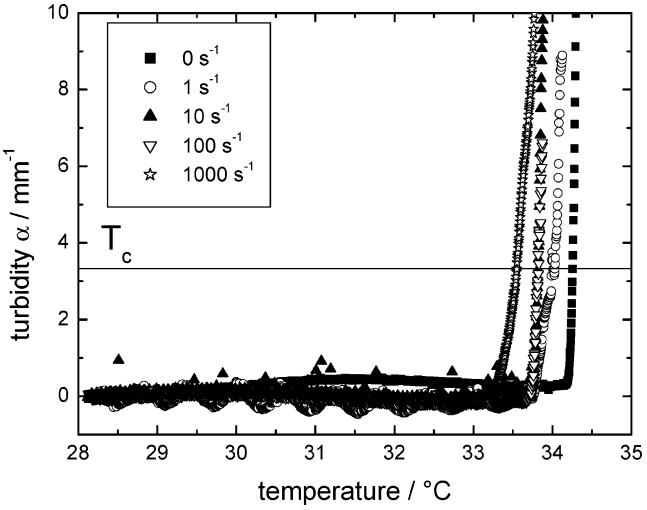


**Figure 6.** Turbidity as a function of temperature for a linear chain PNiPAM solution at 4.0 wt %.

separation for the temperature-sensitive polymers regardless of their macromolecular architecture.

SANS is a further useful technique to study the temperature-induced volume transition in thermosensitive colloidal microgels.[43−47] Crowther et al.[43] describe the temperature-induced deswelling of PNiPAM microgel particles in the $q$ range of 0.01−0.1 Å$^{-1}$. In the swollen state at temperatures below the LCST their data show contributions from polymer chains in a solution-like environment (Ornstein−Zernike scattering). At temperatures above the LCST the scattering profiles exhibit a Porod form ($I \propto q^{-4}$) of scattering relative to the size of the colloidal particles, indicating scattering from a dilute dispersion of noninteracting hard spheres. Dingenouts and co-workers[44−46] report on a continuous volume transition in core−shell particles consisting of a poly(styrene) core and a PNIPAM shell. They demonstrate that the shell has a well-defined compact structure above the LCST. The swelling of the shell is described in terms of an affine expansion of the network, followed by a slight decrease of the volume fraction with increasing distance to the surface of the core. To our knowledge, not much is known about the shear-induced phase separation of thermoresponsive microgels. To gain a more detailed understanding of the shear-induced structures, rheo-SANS experiments were carried out.

First results of the rheo-SANS experiments in the low $q$ regime of a 10.0 wt % PNiPAM microgel at rest and under sheared condition are presented in Figure 7. All scattering patterns remained isotropic even at shear rates of $\dot{\gamma} = 500$ s$^{-1}$ and elevated temperatures. Hence, no deformation of the microgel particles was observed under shear flow. At temperatures well below the LCST (29.2 °C) no significant change in the intensity distribution $I(q)$ is observed when a shear flow is applied. In the quiescent state and under shear the scattered intensity exhibits pronounced form factor minima at the same $q$ values. At temperatures above the LCST (34.4 °C) the PNiPAM microgel suspension demixes. Porod scattering ($I \propto q^{-4}$) is observed in the high $q$ regime as a result of scattering from a sharp interface of the collapsed particle. The scattering profile remains unchanged after shear flow was applied. At temperatures near the LCST (31.5 °C), a strong increase of the scattered intensity is observed when the suspension is

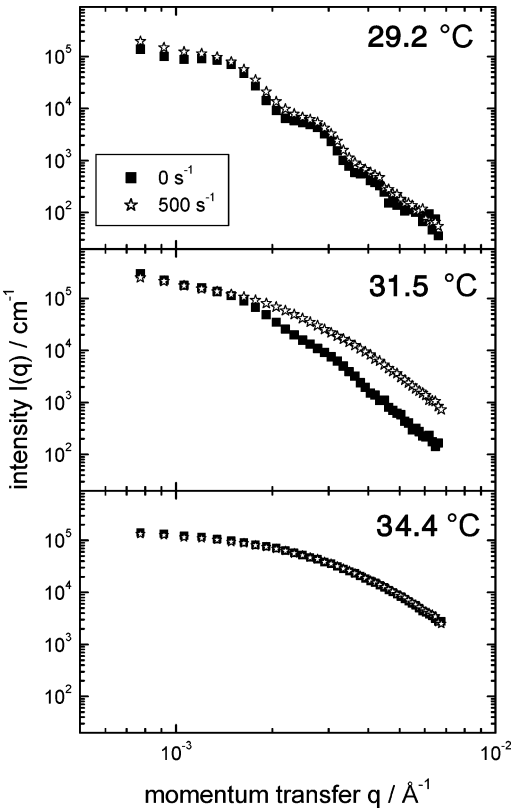


**Figure 7.** SANS scattering intensity distribution $I(q)$ vs momentum transfer $q$ of the PNiPAM microgel at 10.0 wt % for different temperatures at rest and under shear flow. The shear flow strongly influences the form factor at 31.5 °C.

sheared. The minima of the form factor obtained at rest vanish under shear flow, indicating the shear-induced particle collapse. The rheo-SANS studies provided information about the structure of a single particle although the suspensions were highly concentrated (10.0 wt %). For the large particles investigated in this study the main contribution of the scattering in the high $q$ regime arises from the form factor describing the temperature- or shear-induced collapse of a single particle. In contrast, the rheo-turbidity measurements revealed the shear-induced macroscopic phase separation of the concentrated PNiPAM suspensions. Additional rheo-SANS experiments were performed employing PNiPAM microgels with different cross-linking densities and particle sizes, and a detailed fitting model for $I(q)$ was developed in collaboration with Jan Skov Pedersen, University of Aarhus, Denmark. These studies will be presented elsewhere.[38]

Figure 8 displays the cloud curves for both molecular architectures at rest and under sheared conditions. The cloud point temperatures $T_c$ of the microgel are apparently lower than the $T_c$ of the linear PNiPAM. At a concentration of 1.0 wt % the $T_c$ of the microgel ($T_c$ = 32.2 °C) is 1.8 K lower than the $T_c$ of the linear PNiPAM ($T_c$ = 34.0 °C). The cloud point temperatures determined by the onset of a developing turbidity in the rheo-optical experiment are slightly lower than the phase transition temperatures obtained from DSC measurements. Temperatures of 33.6 °C for the microgel and 34.8 °C for the linear polymer were found by DSC in $D_2O$. Otake and co-workers[48] report that the transition temperature of macroscopic PNiPAM gels is always slightly higher (1−2 K) than that of linear PNiPAM solutions. They attribute this effect to the different mobility of the

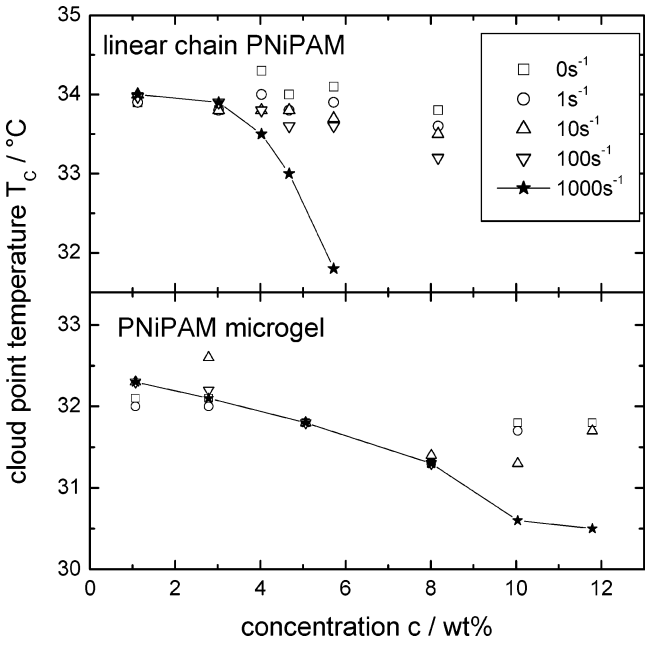


**Figure 8.** Cloud curves of the linear chain PNiPAM (top) and the PNiPAM microgel (bottom) in $D_2O$ at rest and at various shear rates. Shear-induced demixing was observed for both polymer architectures at high concentrations. The lines are guides to the eye.

polymer chains in different molecular architectures and to surface effects of the polymer globule in the solution.

A significant shear-induced shift of $T_c$ is observed only when the polymer concentration was sufficiently high. A shift of 1.0 K was noted for the linear PNiPAM at $\dot{\gamma}$ = 1000 $s^{-1}$ for a concentration of 4.7 wt %. At higher concentrations the effect becomes even more pronounced. For the cross-linked microgel at $\dot{\gamma}$ = 1000 $s^{-1}$ a concentration of 10.0 wt % or higher was required to observe a shift of $T_c$ by 1.2 K. Hence, an influence of shear flow on the miscibility gap was observed only when high Weissenberg numbers ($W_i \equiv \dot{\gamma}\tau$) were applied. A 4.0 wt % solution of the linear PNiPAM at 32 °C exhibits $\tau$ = 0.09 s, and a shift of $T_c$ by 0.8 K was observed when $W_i$ = 90 was reached.

Shear-induced demixing can occur in the PNiPAM/water system independent of the macromolecular architecture. The behavior of the linear PNiPAM in semidilute solution is similar to that of PS in DOP. Shear flow leads to a strong enhancement of concentration fluctuations, and the turbidity rise is observed at lower shear rates when the temperature is closer to the miscibility gap.

Concentrated colloidal suspensions of rigid particles display rich structural changes when strong shear forces are applied. A prominent and technologically important feature is the observation of shear thinning and shear thickening with increasing shear rate, which are related to shear-induced structures including string and bundle like ordering.[49] Verduin et al.[50] investigated the influence of shear flow on the structure of a gel-forming suspension. Stearyl-coated silica particles which behave as sticky hard spheres were suspended in benzene. The phase diagram reveals typical bimodal and spinodal lines, but at high volume fraction the gel line occurs first when the temperature is decreased and the interaction potential becomes more attractive. In rheo-optical experiments an increase of turbidity was observed at very low shear rates, indicating the formation of larger

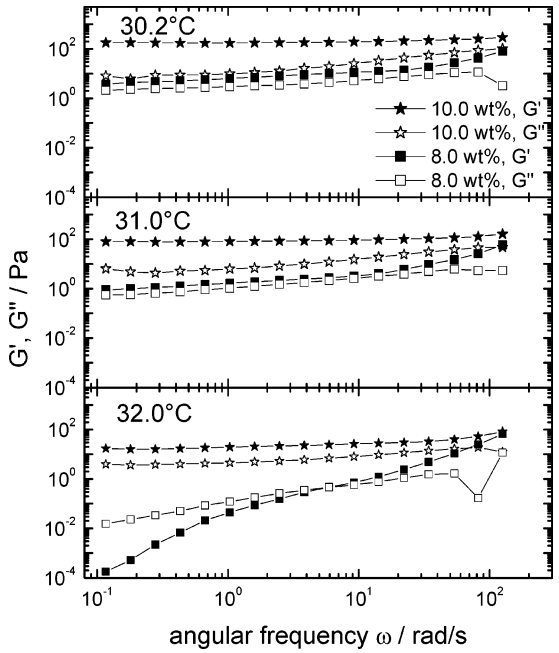


**Figure 9.** Storage modulus $G'$ (filled symbols) and loss modulus $G''$ (open symbols) as a function of angular frequency $\omega$ for the PNiPAM microgel at a concentration of 8.0 and 10.0 wt % at different temperatures. At 32.0 °C, the 8.0 wt % sample is liquid whereas the 10.0 wt % microgel is solid.

structures (mainly along the flow direction). Thus, shear flow destabilized the solution. Higher shear rates, however, shifted the cloud point in the other direction.

The PNiPAM microgel particles investigated in this study have different properties as compared to attractive hard sphere colloids. With increasing temperature the solvent becomes worse, and eventually the interaction potential becomes attractive. Since the microgel particles are swollen by the solvent, the temperature increase also causes the particles to collapse, which does not occur in colloidal suspensions of rigid particles. Therefore, altering the temperature of the thermoresponsive PNiPAM particles leads to changes in the volume fraction as well as interaction potential. Hence, the macroscopic behavior is very different since the liquid to solid transition is shifted to higher concentrations with increasing temperature.

A common feature of the PNiPAM microgel and linear PNiPAM samples is the strong influence of concentration on phase separation under shear. Shear-induced demixing was found at 10.0 wt % but not at 8.0 wt % for the microgel and at 4.0 wt % but not at 3.0 wt % for the linear PNiPAM.

Figure 9 displays results obtained from low-amplitude oscillatory shear experiments for the 8.0 and 10.0 wt % microgel samples. At 30.2 °C both concentrations behave as a viscoelastic solid, and the storage modulus is larger than the loss modulus. Near the equilibrium cloud temperature the two samples reveal a characteristic difference in the viscoelastic properties. At 32.0 °C the lower concentrated sample behaves as a viscoelastic liquid, and the loss modulus exceeds the storage modulus. The 10.0 wt % sample, however, revealed a dominant elastic behavior. This indicates that the presence of an elastic material with a close packing of particles is necessary in order to influence the phase separation process by shear flow.

The temperature-dependent solid−liquid transition can also be detected by dynamic light scattering (DLS). The transition from a nonergodic to an ergodic system is revealed in the decay of the time correlation function (TCF) and the speckle pattern. At 32.3 °C the 8.0 wt % sample displays a monoexponential decay of the TCF which is no longer observed with the 10.0 wt % sample. Hence, the 8.0 wt % suspension is liquid and the 10.0 wt % sample solid at 32.3 °C. The DLS experiments are in good agreement with the rheological experiments.

The observation that the cloud curve is only affected by shear flow when the sample has dominant elastic properties indicates that the shear-induced phase separation process is not only related to the attractive interaction potential of the microgel particles. Even at a concentration of 8 wt % the shear flow reached the limit of high Peclet numbers and should be sufficient to induce particle collisions and aggregation. Instead, it appears that a solvent squeezing mechanism is responsible for the shear-induced demixing at high concentration. The coupling between concentration fluctuations and shear stress in entangled polymer solution can lead to stress relaxation via solvent squeezing.[51]

A similar mechanism can be suggested for microgel particles if the particles are densely packed such that relaxation via particle diffusion is hindered. The long time self-diffusion of the particles is strongly suppressed above the liquid−solid transition. However, in contrast to rigid particles, the microgel particles can be compressed. Thus, a coupling between the shear stress and fluctuation in the local packing density can result in squeezing of solvent, giving rise to an enhancement of concentration fluctuations and turbidity.

It should be noted that shear-induced demixing was observed not only for the microgel presented here but also for a PNiPAM microgel with the same cross-linking density (1.5 mol %) but smaller particle size. In contrast, for a PNiPAM microgel with a higher degree of cross-linking density (5.5 mol %) shear-induced demixing was not observed. The solvent inside the particle seems to be immobilized because of the high cross-linking density. The particles cannot be compressed as much as the particles with a lower degree of cross-linking, and stress relaxation through solvent squeezing might be hindered. The increase of turbidity with increasing temperature is related to an aggregation of the particles.

## 4. Conclusions

Rheological properties of aqueous solutions of linear PNiPAM and of PNiPAM microgel particles were studied. The flow behavior and the viscoelastic properties of the linear polymer solutions revealed no pronounced temperature dependence. As along as the concentration stays well above the overlap concentration, the rheological properties are not very sensitive to temperature-induced changes in the size of an individual macromolecule. In contrast, a pronounced influence of temperature on those rheological properties was found for the microgel, since the effective volume fraction which determines flow and viscoelastic behavior strongly depends on temperature. A scaling behavior of the characteristic relaxation time of the linear PNiPAM with concentration is described.

Shear-induced phase separation was observed for aqueous solutions of linear PNiPAM and of PNiPAM microgel particles. The cloud curve was shifted to lower temperatures with increasing shear rate. With the microgel system with a cross-linking density of 1.5 mol %, an influence of shear flow on the turbidity was only

observed when the particle density was sufficiently high to be above the liquid−solid transition. This indicates that a coupling of shear stress with the concentration fluctuations leading to solvent squeezing is only possible when the particles are densely packed. For a PNiPAM microgel with a higher degree of cross-linking (5.5 mol %) shear-induced demixing was not observed. Stress relaxation through solvent squeezing might be hindered since the particles cannot be compressed as much as the ones with a lower degree of cross-linking.

**Acknowledgment.** Financial support by the Deutsche Forschungsgemeinschaft and the Fonds der Chemischen Industrie is gratefully acknowledged. We thank Jaro Ricka and Rene Nyffenegger, University of Berne, Switzerland, for the possibility to synthesize the linear PNiPAM in their lab. We thank Peter Lindner, Institute Laue-Langevin, Grenoble, France, for his support with the SANS experiments at the D11 beamline.

## References and Notes

(1) Schild, H. G. *Prog. Polym. Sci.* **1992**, *17*, 163.
(2) Klug, E. D. *J. Polym. Sci., Part G* **1971**, *36*, 491.
(3) Eisele, M.; Burchard, W. *Makromol. Chem.* **1990**, *191*, 169.
(4) Pelton, R. *Adv. Colloid Interface Sci.* **2000**, *85*, 1.
(5) Dhara, D.; Chatterji, P. R. *Rev. Macromol. Chem. Phys.* **2000**, C*40*, 51.
(6) Saunders, B. R.; Vincent, B. *Adv. Colloid Interface Sci.* **1999**, *80*, 1.
(7) Kawasaki, H.; Sasaki, S.; Maeda, H. *J. Phys. Chem. B* **1997**, *101*, 4184.
(8) Zhang, Y. Q.; Tanaka, T.; Shibayama, M. *Nature (London)* **1992**, *360*, 142.
(9) Inomata, H.; Wada, N.; Yagia, Y.; Goto, S.; Saito, S. *Polymer* **1995**, *36*, 875.
(10) Shibayama, M.; Fujikawa, Y.; Nomura, S. *Macromolecules* **1996**, *29*, 6535.
(11) Rangel-Nafaile, C.; Metzner, A. B.; Wissbrun, K. F. *Macromolecules* **1984**, *17*, 1187.
(12) Morfin, I.; Lindner, P.; Boué, F. *Macromolecules* **1999**, *32*, 7208.
(13) Saito, S.; Hashimoto, T.; Morfin, J.; Lindner, P.; Boué, F. *Macromolecules* **2002**, *35*, 445.
(14) Saito, S.; Hashimoto, T. *J. Chem. Phys.* **2001**, *114*, 10531.
(15) Bastide, J.; Leibler, L.; Prost, J. *Macromolecules* **1990**, *23*, 1821.
(16) Moses, E.; Kume, T.; Hashimoto, T. *Phys. Rev. Lett.* **1994**, *72*, 2037.
(17) DeGroot, J. V.; Macosko, C. W.; Kume, T.; Hashimoto, T. *J. Colloid Interface Sci.* **1994**, *166*, 404.
(18) Belzung, B.; Lequeux, F.; Vermant, J.; Mewis, J. *J. Colloid Interface Sci.* **2000**, *224*, 179.
(19) Weigel, R.; Läuger, J.; Richtering, W.; Lindner, P. *J. Phys. II* **1996**, *6*, 529.
(20) van Egmond, J. W. *Macromolecules* **1997**, *30*, 8045.
(21) Pönitsch, M.; Hollfelder, T.; Springer, J. *Polym. Bull. (Berlin)* **1998**, *40*, 345.
(22) Badiger, M. V.; Lutz, A.; Wolf, B. A. *Polymer* **2000**, *41*, 1377.
(23) Schmidt. J.; Burchard, W.; Richtering, W. *Biomacromolecules* **2003**, *4*, 453.
(24) Badiger, M.; Wolf, B. A. *Macromol. Chem. Phys.*, in press.
(25) Wolf, B. A. *Macromolecules* **1984**, *17*, 615.
(26) Helfand, E.; Fredrickson, G. H. *Phys. Rev. E* **1989**, *62*, 2468.
(27) Milner, S. T. *Phys. Rev. E* **1993**, *48*, 3674.
(28) Onuki, A. *J. Phys.: Condens. Matter* **1997**, *9*, 6119.
(29) Vermant, J.; Raynaud, L.; Mewis, J.; Ernst, B.; Fuller, G. G. *J. Colloid Interface Sci.* **1999**, *211*, 221.
(30) Meewes, M.; Ricka, J.; de Silva, M.; Nyffenegger, R.; Binkert, Th. *Macromolecules* **1991**, *24*, 5811.
(31) Kulicke, W.; Klein, J. *Angew. Makromol. Chem.* **1987**, *69*, 169.
(32) Senff, H.; Richtering, W. *J. Chem. Phys.* **1999**, *111*, 1705.
(33) Senff, H. PhD Thesis, University of Freiburg, Germany, 1999.
(34) Zipfel, J.; Berghausen, J.; Schmidt, G.; Lindner, P.; Tsianou, M.; Alexandridis, P.; Richtering, W. *Phys. Chem. Chem. Phys.* **1999**, *1*, 3905.
(35) Kubota, K.; Fujishige, S.; Ando, I. *Polym. J.* **1990**, *22*, 15.
(36) Wu, C. *Polymer* **1998**, *39*, 4609.
(37) Hansen, J. C.; Maier, D.; Honerkamp, J.; Richtering, W.; Horn, F. M.; Senff, H. *J. Colloid Interface Sci.* **1999**, *215*, 72.
(38) Stieger, M.; Pedersen, J. S.; Lindner, P.; Richtering, W. Manuscript in preparation.
(39) Shirota, H.; Endo, N.; Horie, K. *Chem. Phys.* **1998**, *238*, 487.
(40) Cox, W. P.; Merz, E. H. *J. Polym. Sci.* **1958**, *28*, 619.
(41) Cross, M. *J. Colloid Sci.* **1965**, *20*, 417.
(42) Elias, H. G. In *Makromoleküle Band 2*, 6th ed.; Wiley-VCH Verlag: Weinheim, Germany, 2001; p 395.
(43) Crowther, H. M.; Saunders, B. R.; Mears, S. J.; Cosgrove, T.; Vincent, B.; King, S. M.; Yu, G. E. *Colloids Surf. A* **1999**, *152*, 327.
(44) Dingenouts, N.; Seelenmeyer, S.; Deike, I.; Rosenfeldt, S.; Ballauff, M.; Lindner, P.; Narayanan, T. *Phys. Chem. Chem. Phys.* **2001**, *3*, 1169.
(45) Seelenmeyer, S.; Deike, I.; Rosenfeldt, S.; Norhausen, Ch.; Dingenouts, N.; Ballauff, M.; Narayanan, T.; Lindner, P. *J. Chem. Phys.* **2001**, *114*, 10471.
(46) Dingenouts, N.; Norhausen, Ch.; Ballauff, M. *Ber. Bunsen-Ges. Phys. Chem.* **1998**, *102*, 1594.
(47) Hellweg, T.; Dewhurst, C. D.; Brückner, E.; Kratz, K.; Eimer, W. *Colloid Polym. Sci.* **2000**, *278*, 972.
(48) Otake, K.; Inomata, H.; Konno, M.; Saito, S. *Macromolecules* **1990**, *23*, 283.
(49) Hess, S.; Loose, W. *Rheol. Acta* **1989**, *28*, 91.
(50) Verduin, H.; de Gans, B. J.; Dhont, J. K. G. *Langmuir* **1996**, *12*, 2947.
(51) Saito, S.; Koizumi, S.; Matsuzaka, K.; Suehiro, S.; Hashimoto, T. *Macromolecules* **2000**, *33*, 2153.

MA034788S